ACS APPLIED MATERIALS & INTERFACES

Spotlight on Applications

www.acsami.org

Boron Subphthalocyanines as Organic Electronic Materials

Graham E. Morse[†] and Timothy P. Bender*[,†,‡,§]

[†]Department of Chemical Engineering and Applied Chemistry, The University of Toronto, 200 College Street, Toronto, Ontario, Canada M5S 3E5

[‡]Department of Chemistry, University of Toronto, 80 St. George Street, Toronto, Ontario, Canada M5S 3H6

[§]Department of Materials Science and Engineering, University of Toronto, 184 College Street, Toronto, Ontario, Canada M5S 3E4

ABSTRACT: Boron subphthalocyanines (BsubPcs) are an emerging class of high performing materials in organic electronics. Since the first use of chloroboron subphthalocyanine in an organic electronic device 6 years ago subphthalocyanines have shown potential as functional materials in organic light emitting diodes (OLEDs) and organic photovoltaics (OPVs). Here we review the material properties of chloroboron subphthalocyanine (Cl-BsubPc) and its use as an organic semiconductor. We then highlight our efforts toward derivatives of boron subpthalocyanine beyond Cl-BsubPc and discuss the impact of molecular design on the material properties and the performance of the BsubPc. Finally, we comment on the status of BsubPcs in the field of organic electronics and discuss how we believe future progress can be made.

KEYWORDS: *boron, subphthalocyanine, organic, solar cell, light emitting diode, transistor, design, photovoltaics, review*

INTRODUCTION

The exploration of organic electronics began more than 60 years ago with the pioneering work of xerographists in electrophotography (later termed xerography),[1] with physicists studying the electronics of organic materials,[2] and electrochemists studying electrogenerated chemiluminescence[3] and photogalvanics.[4] Modern solid state organic electronic devices such as organic light-emitting diodes (OLEDs) were initially developed by Tang in the industrial research laboratories of Kodak in the 1980s.[5,6] Since then, organic alternatives to inorganic semiconductors have been developed and incorporated into a variety of electronic devices besides OLEDs including thin film transistors (OTFTs) and photovoltaic cells (OPVs or organic solar cells). Improvements in device performance have been achieved through the development of new device architectures and through the rational design of new organic or inorganic/organic functional/active materials (or compositions of matter). Although modern chemical synthesis techniques do provide a set of powerful tools for molecular manipulation, for the creation of entirely new aromatic systems, for the re-engineering of known aromatic systems, and for the incorporation of underutilized elements into organic electronic materials, challenges still remain. One could argue that the development of novel functional materials has not kept pace with novel device designs and architectures. Aptly selecting materials as synthetic targets based on criteria needed for application into a particular device is major consideration in material design: it requires an understanding of physical chemical properties, solid state organization, and molecular level electronics. Learning from a particular class of materials, can add to the understanding of molecular design challenges and targets, contributing to the selection of future material classes.

In this Spotlight on Applications, we aim to use boron subphthalocyanines (BsubPcs) as a case study to underline their unique properties and the challenges involved in the use of an emerging class of organic semiconductors. In particular, we will present to the readers the synthesis of BsubPcs, detail their unique physiochemical properties, inform on the current status of electronic devices fabricated in part by this class of material, and provide insight into their future applications through molecular design, most notably by outlining the need to move beyond the most basic BsubPc derivative Cl-BsubPc. We will broadly segment this analysis into four sections each focusing on the molecular and physical chemical properties, bulk material properties, and device performance/properties of BsubPcs, finishing with a commentary on synthetic methods leading to novel derivatives.

BORON SUBPHTHALOCYANINE

Phthalocyanines (Pc) discovered by Dandridge and Dunsworth in 1928[7] are a class of common colorants that have also been employed as functional materials in organic electronic devices.[5,8] They contain a central metal atom surrounded by a tetrameric ligand formed of nitrogen-linked isoindoline units commonly referred to as diiminoisoindoline units (Figure 1a). The four central nitrogen atoms ligate the metal ion in the central cavity via two covalent and two coordination bonds.

Received: July 31, 2012
Accepted: September 17, 2012
Published: September 17, 2012

   dx.doi.org/10.1021/am3015197 | *ACS Appl. Mater. Interfaces* 2012, 4, 5055−5068

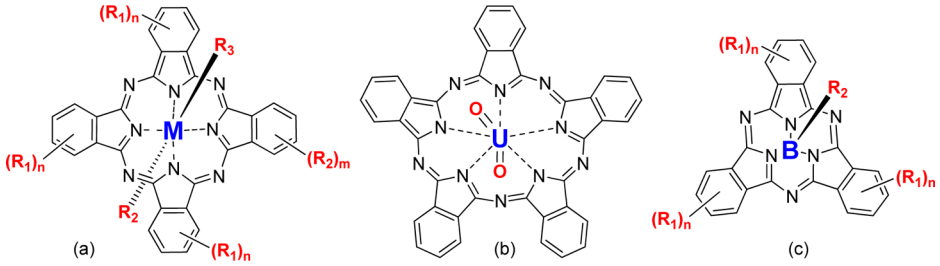

Figure 1. Chemical structure of (a) generic phthalocyanines, (b) uranyl superphthalocyanine, and (c) boron subphthalocyanine.

Virtually all metal and metaloid atoms of the periodic table form Pcs by actively templating the formation of the ligand structure during reaction of phthalonitrile (or phthalonitrile derivative) with the respective metal halide (or metal alkoxide). The two exceptions are uranium and boron, which form uranyl superphthalocyanine[9] (Figure 1b) and boron subphthalocyanine[10] (Figure 1c), which have five and three repeating isoindoline units in their ligand structure respectively. Boron has the smallest atomic radius of all metals and metaloids in the periodic table. This, combined with its oxidative state of 3+, presumably templates the formation of the smaller trimeric homologue of Pc.[11] Structurally, the boron atom is chelated by the three pyrrole nitrogens (N_p, Figure 2a). Each isoindoline

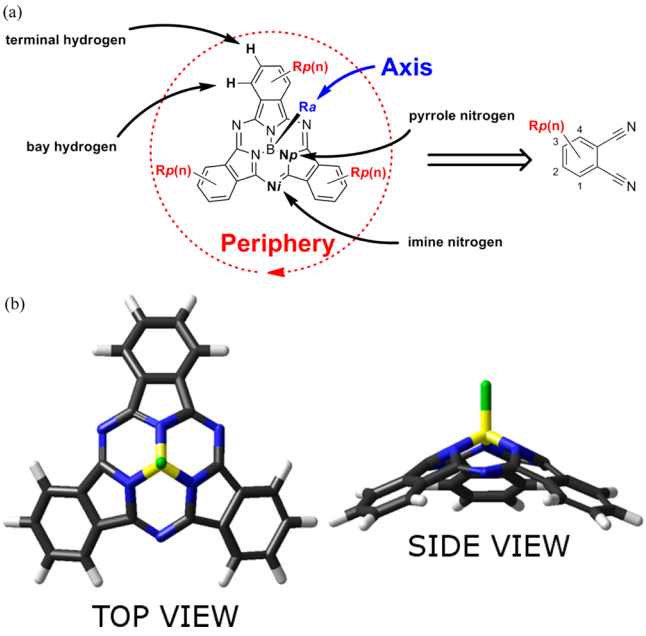

Figure 2. (a) BsubPc molecular structure with descriptive terminologies highlighted. (b) 3D structure of Cl-BsubPc illustrating its unique bowl-shaped structure.

fragment is joined by an imine nitrogen (N_i) forming the repeating diiminoisoindoline unit and the aromatic 14 π-electron system of the subPc ligand. The atomic radius of boron is slightly larger than the cavity causing the subPc ligand to adopt a nonplanar conformation (Figure 2b). If the N_p nitrogen atoms are used to define a plane (the *xy*-plane) then all of the atoms making up the macrocycle are present below this plane. The resulting geometry is often referred to as a "bowl" or "cone", the former being preferred. A bond to the boron atom protrudes from the convex side of the bowl which is referred to as the axial bond (R_a) and defines a *z*-axis. The BsubPc molecular fragment and any axially substituted monatomic derivatives (namely fluoro-, chloro-, and bromo-BsubPc) possess C_{3v} symmetry. The outer edge of the BsubPc molecular fragment commonly contains 12 hydrogen atoms and is termed the periphery of the molecule (R_p). These hydrogens are available for substitution by direct modification of the phthalonitrile prior to BsubPc formation[12,13] or by post modification.[14] Functional groups present in the 1,4 positions of the phthalonitrile yields substitution in the bay position, whereas the same in the 2,3 position produces terminal substitution; and tetrasubstituted phthalonitrile yields a completely substituted periphery. A mono-, di-, or trisubstitution pattern results in the formation of isomers and breaks the C_{3v} symmetry,[13,15] which can create practical challenges during product isolation and purification.[16] Within the text of this Spotlight, we will use a systematic naming scheme with reference to Figure 1 to describe the various BsubPc derivatives. For example, Cl-BsubPc refers to $R_p(12)$ = H and R_a = Cl; PhO-BsubPc refers to $R_p(12)$ = H, R_a = OC_6H_6; Cl−Cl_6BsubPc refers to $R_p(6)_{1,4}$ = H, $R_p(6)_{2,3}$ = Cl, R_a = Cl, and so on.

MOLECULAR PHYSICAL CHEMICAL PROPERTIES OF BSUBPCS

The π-electron configuration of an organic or inorganic/organic material is of paramount importance for its application as an active material in OLEDs and OPVs. The symmetrical 14 π-electron system of BsubPcs both absorbs and emits radiation in the visible spectrum (Figure 3). Their most prominent and lowest energy absorption band, known as the Q-band, is seen generally between 560−600 nm equating to an optical band gap of 2.1−2.0 eV. It results from the C_{3v} symmetric BsubPc ligand/molecular fragment which has an inherent degeneracy between the LUMO and LUMO^{+1}. Degeneracy in these orbitals dictates the allowed electronic transitions which

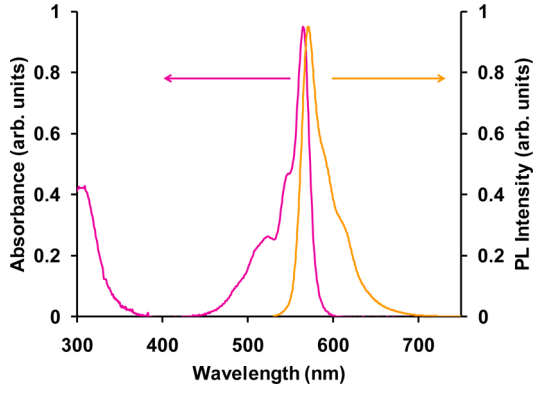

Figure 3. Absorption (magenta) and emission (orange) spectrum of Cl-BsubPc in toluene.

dx.doi.org/10.1021/am3015197 | ACS Appl. Mater. Interfaces 2012, 4, 5055−5068

contribute to the Q-band − excitation from the equivalent HOMO/HOMO^{-1} to the LUMO and the LUMO^{+1}. Their high symmetry also contributes to a high molar extinction coefficient (ε)[17] typically between 50 000 and 80 000 M^{-1} cm^{-1}.[15,18,19] A shoulder to the blue side of the Q-band and a UV absorption below 400 nm are also characteristic of BsubPcs.

The prototypical Cl-BsubPc contains a small permanent dipole moment in the z-plane. BsubPcs have been theoretically predicted to experience a minimal change in this dipole upon excitation suggesting that little or no reorganization takes place.[20] This is experimentally consistent with the minimal solvent effects and small Stokes shifts observed. Generally for BsubPcs different solvents cause only a minimal shift of 1−2 nm in the Q-band depending on solvent polarity (molecules which experience a large transition dipole moment experience greater solvent effects)[21] and likewise small changes in Stokes shifts are observed between 8 and 30 nm[19,22−24] (dependent on the reorganization energy of BsubPcs in solvent upon excitation).[25] The fluorescence spectrum of BsubPcs typically shows a narrow emission (30 to 60 nm width at half height) yielding a red-orange emission with a peak max between 580 and 620 nm (shown in Figure 3 for Cl-BsubPc). The presence of emission peaks ranging from 620 to 720 nm is possible with the route cause determined to be molecular aggregation and emission from that aggregate.[22,24] Although aggregate emission can pose color purity issues in OLEDs, strategies have been developed to prevent aggregate formation and the subsequent photoemission from the aggregate.[22]

Frontier molecular orbitals (HOMO, HOMO^{-1}, LUMO, and LUMO^{+1} for example) not only define the optical transitions for a molecule but also their absolute position defines their functionality in organic electronic devices. A high π-character, approximately 70% for LUMOs and 80% for HOMOs,[26] is observed for BsubPc derivatives with these orbitals residing on the π aromatic surface of the BsubPc molecular fragment (Figure 4). The frontier molecular orbitals for halo-BsubPcs display a minimal response in their spatial distribution and their energy levels with variation in the axial substituent.[15,27] There are three main factors which contribute to the electronic disconnection between the axial substituent and the BsubPc macrocycle: (1) the BsubPc molecular fragment curves away from the axial fragment which protrudes perpendicularly from the tetra-coordinated boron atom spatially isolating the axial fragment,[28] (2) an orbital density node appears on the boron atom in the frontier orbitals in BsubPcs,[29,13] and (3) the local C_{3v} symmetry and degeneracy of the BsubPc molecular fragment is preserved upon axial modification, regardless of the nature of the axial ligand.[30] Consequently, axial modification has little impact on the Q-band peak location, absorption peak shape and absolute molecular orbital energy levels of halo-BsubPcs[13] including in the case where the axial position is occupied by an extended π-system.[31]

A popular route to estimate the HOMO and LUMO energy levels of organic compounds is through the measurement of electrochemical oxidation and reduction potentials, specifically using cyclic voltammetry (CV) or differential pulse voltammetry. In the literature, BsubPc derivatives have consistently been observed to have irreversible oxidation and reduction events under cyclic voltammetry conditions, despite many efforts exploring various synthetic derivatives, solvents (ACN, THF, or DCM), electrolytes (Bu_4NPF_6, or Bu_4NClO_4) and electrodes (glassy carbon, gold, or platinum). Often this irreversibility occurs during their oxidation while the reduction events are equally probable to be reversible or irreversible.[23] This suggests that BsubPc derivatives are more stable as radical anions than as radical cations and that BsubPc derivatives may be more suitable as n-type materials (also referred to as acceptor materials and/or electron transport materials).[24,32−34] Ultraviolet photoemission spectroscopy (UPS) and inverse photoelectron spectroscopy (IPES) are common approaches used to

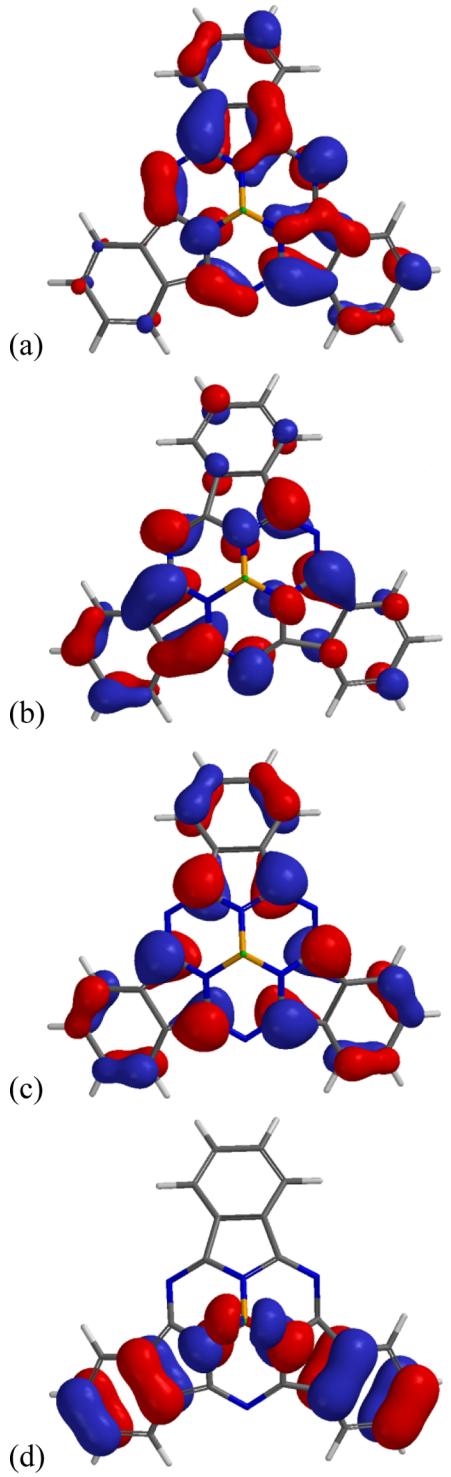

Figure 4. (a) LUMO+1, (b) LUMO, (c) HOMO, and (d) HOMO-1 distribution for Cl-BsubPc calculated using DFT B3LYP (6-31G* basis set).

dx.doi.org/10.1021/am3015197 | ACS Appl. Mater. Interfaces 2012, 4, 5055−5068

measure ionization potential and electron affinity of a thin solid film (respectively) which have been shown to estimate frontier orbital energy levels. The HOMO of Cl-BsubPc has been estimated by UPS as 5.7 eV[35] and 5.65 eV[36] or by CV as 5.6 eV (LUMO 3.6 eV)[37] and 5.5 eV (LUMO 3.4 eV).[32] Other halides such as Br-BsubPc and F-BsubPc have been shown by CV to shift the oxidation potential by +0.05 V and −0.05 V respectively.[38] The HOMO and LUMO of other peripheral derivatives of Cl-BsubPcs have been estimated exclusively by CV and are summarized in Figure 5.[32,39,40] A large variation in electrochemical redox is observed for the different peripheral derivatives varying by ∼0.7 V between Cl-tBu$_3$BsubPc[39] and Cl−F$_{12}$BsubPc.[40]

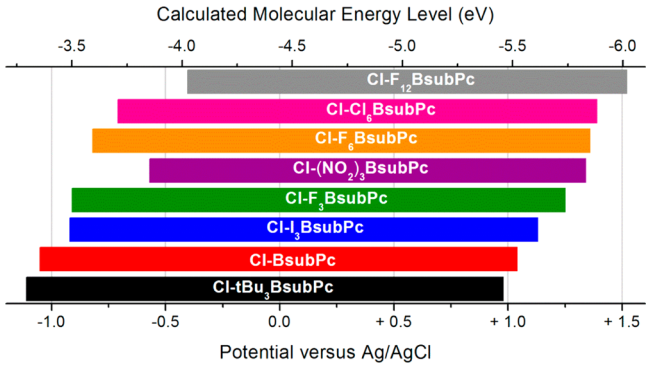

Figure 5. Oxidation and reduction half-wave potentials for a series of peripheral chloro-BsubPc derivatives. Each BsubPc undergoes irreversible oxidation and reduction events with the exception of Cl−F$_{12}$BsubPc, which undergoes a reversible reduction.[32,39] The exact molecular structures of each BsubPc are described in the abbreviation list accompanying this article. Note: each BsubPc was measured in dichloromethane and referenced to Ag/AgCl in saturated sodium chloride except for Cl−F$_{12}$BsubPc, which was reportedly measured in THF with reference to ferrocene/ferrocenium. A rough estimate of the molecular energy levels for these materials has been made from the following equation: $E_{HOMO} = 4.4 + E_{CV}$.[114]

BULK MATERIAL PROPERTIES

Organic electronic devices are composed of layers of thin solid films of functional organic materials. Regardless of the deposition method, the properties of these films are obviously critical to their proper function in devices. The properties of the thin solid film are dictated by the molecular properties described above combined with the translation of the molecular properties into the solid state wherein intermolecular interactions can perturb each molecular property in a way that is not entirely predictable. As such, the changes in photophysical or electrophysical properties on moving to a bulk film must be understood as an integral aspect of device engineering. Additionally, molecular properties such as solubility and thermal stability play a role in the ability to form thin solid films in a suitable configuration for functioning in a specific device. In this section, we will thus highlight the properties of BsubPcs, enabling the formation of bulk thin solid films and the resulting properties of said films.

Two routes exist for fabricating functional organic layers in modern organic electronic devices: (1) solution deposition by solubilizing the functional organic material in a selected solvent and (2) deposition of the functional organic material by sublimation under high vacuum conditions. Thus a detailed understanding of solubility and thermal stability must be developed for each class (whether new or existing) of organic electronic materials. The solubility of Cl-BsubPc has been reported and is low (∼1 × 10^{-4} M on average in a selection of seven solvents).[18] Similar solubility is observed for other halo-BsubPcs and this low solubility has limited their application as solution deposited films in organic electronic devices. Exceptions are seen when solubilizing peripheral substituents are present including $R_p(12)$ = −F,[41] −OCH$_2$CF$_3$,[42] $R_p(6)_{2,3}$ = 15-crown-5,[43] and $R_p(3)_2$ = −OCH(CH$_2$(CH$_3$)$_2$)$_2$.[44] The sublimability of BsubPc materials has not been systematically studied however a large collection of BsubPc derivatives have been reported to form bulk films on sublimation. Halo-BsubPcs, such as Cl-BsubPc, Cl−Cl$_6$BsubPc, Cl−F$_3$BsubPc, Cl−F$_6$BsubPc, Cl−F$_{12}$BsubPc, and F−F$_{12}$BsubPc, are generally sublimable.[32,34,37]

Bulk film properties have been reported for Cl-BsubPc and two fluorinated derivatives, Cl−F$_{12}$BsubPc and F−F$_{12}$BsubPc.[34] Their refractive index changes with molecular structure from a high of 1.62 for Cl-BsubPc to a lower value for the fluorinated derivatives (0.64 and 0.92, for F$_{12}$BsubPc and F−F$_{12}$BsubPc respectively). A dielectric constant for Cl-BsubPc was found to be 3.9 while a significantly lower value was measured for the fluorinated derivatives F$_{12}$BsubPc and F−F$_{12}$BsubPc (2.3 − 3.3 respectively).[34,45] For comparison most organic materials are assumed to have a dielectric constant near 3.0 and is one of their limiting factors.

The observation of submonolayer behavior of a material on a surface can explicate molecular interactions and/or template film growth effecting properties observed in thicker bulk films.[46] The growth of thin submonolayer films of Cl-BsubPc has been studied by STM, SEM and LEED.[47−50] On surfaces, Cl-BsubPc displays orientation effects specific to the nature of the underlying material. Materials studied include highly regular surfaces of Si, Ag, Au and Cu. On Si(111) Cl-BsubPc situates on restatoms with the Cl−B bond pointing toward the surface (Cl-down).[48] Its close proximity and interaction between the highly polar dangling Si bonds with the imine nitrogens around the BsubPc led to the observation of decomposition of the BsubPc macrocycle into smaller molecular fragments.[48] On Ag(111) surfaces, Cl-BsubPc also points its axial chloride toward the surface. A detailed investigation of the surface by STM found a reorganization from a 2D lattice, to a honeycomb pattern upon a change in surface coverage from 0.2 monolayers to 0.5 monolayers at room temperature[51] showing multiple solid-state polymorphs that were computationally verified.[52] While adsorbed, the BsubPc remains intact, and the molecules were shown to be mobile on the surface. They were also found to be mobile within the gas phase.[50] On Au(111) surfaces, Cl-BsubPc is also mobile resulting in the formation of well-ordered arrangements beyond 1 monolayer of coverage. No islanding is observed for the first monolayer and the BsubPc orients with its chlorine atom pointing away from the surface (Cl-up) and its three imine nitrogen atoms attached to the surface[47] or with its chlorine atom pointing toward the surface (Cl-down).[53] On Au surfaces, four different phases of surface coverage have been reported for Cl-BsubPc: honeycomb, diamond, intermediate and hexagonal close packed.[53] On Cu(100), similar to Au, both the Cl-up and Cl-down orientations were observed by STM.[49] Interestingly, the applied bias for STM imaging can affect the orientation of these molecules causing them to change orientation, although fine control of a single molecule is not possible because of intermolecular entanglement.[54]

Beyond the monolayer, BsubPc thin films are consistently reported to be conformal, exhibiting low rms surface roughness between 0.4−5.0 nm.[34,55,56] Despite their conformal and often amorphous appearance, long-range organization and/or crystallinity in these films has been reported by X-ray crystal diffraction.[45,,56] The combination of crystalline yet conformal film formation is advantageous to device fabrication. The fine texture of the films creates a larger surface area for charge separation,[56] the conformal nature prevents pinholes and shorts, and the crystallinity should lead to high charge transport in these films.[57]

Certain chemical species have unique interactions with BsubPcs. In particular fluoride,[58] cyanide,[59] Lewis acidic aluminum halides or phenoxides,[60] Lewis acidic boron halides,[61] NPB[62] and C_{60}[63] have been show to exhibit specific interactions involving complexation or charge transfer. In some cases these interactions have been exploited in devices, but in other examples, the effects are not beneficial.

The high degree of variability in polymorphism, molecular mobility, orientation, and stability seen by STM by various researchers suggests that BsubPcs interactions with surfaces are variable and case specific. This combined with the ability of BsubPcs to interaction with other organic or inorganic chemicals/compounds indicates to the authors that close attention should thus be paid to its interactions with materials more common to organic electronics such as ITO, Al, LiF, MoO_3, and adjacent organic materials commonly used in devices.

The stability of BsubPcs can be and has been characterized in terms of both photostability (photo-oxidative stability) and thermal stability. Each of these measurements is valuable in different aspects of our understanding of molecular stability. Thermal stability should be taken into account when a robust molecular structure is required for vacuum deposition techniques to be used or for when it is to be placed in an environment with variable temperatures, for example, in an organic solar cell. The overall thermal stability is a reflection of its weakest bond. For BsubPcs the rigid aromatic BsubPc fragment is thermally stable whereas the exposed and labile axial ligand is the weakest link. This was demonstrated by González-Rodríguez et al. who measured the thermal stability of a series of different axial BsubPcs: Br-BsubPc, Cl-BsubPc, HO-BsubPc, and PhO-BsubPc.[64] For each of these materials their degradation point was above 300 °C and thus all are thermally robust. The first degradation product is the cleavage of the axial ligand which occurs on the order of Br < OH < Cl∼OPh. Peripheral modifications were shown to effect the stability to a lesser extent although only singly substituted phthalonitriles were compared (terminal substitution $R_p(3)_2$ = $-NO_2$, −I, and −OPh).

Yamasaki and Mori also compared the thermal and photostability of peripheral and axial derivatives after a week of simulated environmental testing.[65] Similar to the report of González-Rodríguez et al., they found that rigid axial bonds where more stable (OPh < Cl < Ph). They compared aryl and alkyl thiol peripheral substitution (terminal $R_p(6)$ = −H, −S-isopentyl, and −SPh) and found that moderate electron-withdrawing peripheral aryl and alkyl thiols substituents to best impact photostability, whereas the more rigid −SPh and −H showed the best thermal stability.

Our group has studied the photostability of a series of highly soluble BsubPc derivatives doped into thin films of polystyrene, under ambient conditions and natural sunlight. We compared the effect of axial and peripheral substitution on molecular stability[66] and found that the axial ligand has a minimal effect on stability, whereas peripheral substitution greatly impacted photostability. When the electron-withdrawing fluorine-group was present around the periphery, the photostability was greatly enhanced compared to derivatives with hydrogen- or electron-donating substituents (phenyl ethers in this case).

Within a functional organic electronic device, a given material will undergo trillions of oxidation or reduction events over its lifetime. Thus, electrochemical reversibility is a third measure of stability relevant to the application of a material in organic electronic devices as it can indicate the stability of the reduced or oxidized form of a material. Ferro et al. reported on the effects of charge on the molecular structure of Cl-BsubPc.[67] They found that when negatively or positively charged the axial B−Cl bond extends whereas the other bonds within the BsubPc showed no significant change. This would suggest that the axial substituent is most susceptible to cleavage when charged, and as a corollary, the nature of the axial substituent should greatly impact its redox stability (the stability of the radical anion or radical cation). In a recent paper our group summarized the general electrochemical reversibility of BsubPc derivatives reported in literature.[23] Generally most BsubPcs show reversible reductions and irreversible oxidations (Figure 5). Indeed, there are some classes of axial substituents that impart bipolar redox stability, namely, phth-BsubPc[23] and alkynyl-BsubPcs.[68]

Other aspects of environmental stability include hydrolytic stability. This is of a lesser concern as organic electronic devices are generally encapsulated and thus insulated from water. Nonetheless, the reaction of halo-BsubPcs with water is known and well-reported.[69−71] However, replacing the axial halogen of a halo-BsubPc with a nucleophile passivates the BsubPc towards moisture.[71]

Crystallization of BsubPcs is readily achieved using sublimation, liquid−liquid layering and vapor diffusion techniques.[72] In the solid state, BsubPcs tend to orient based on strong interactions between the BsubPc molecular fragments however peripheral halogenation can drastically alter this preference leading to BsubPc interactions with the axial fragment forming ribbons or columns.[24,61,72] There is a body of research which correlates the crystal packing of functional organic materials with their respective charge carrier mobility.[73] For BsubPcs, this correlation has not yet been thoroughly examined although we have shown a general correlation between solid state packing density and charge transport for thin films of fluorinated phenoxy-BsubPcs.[45] In this paper, we measured the electron mobility of a series three fluorinated phenoxy-BsubPcs to be on the order of 1×10^{-4} to 1×10^{-5} $cm^2\ V^{-1}\ s^{-1}$, with a field dependence that we correlated to the solid state arrangement (further discussed later in this Spotlight).[45] This is significantly higher than the charge transport mobility of Cl-BsubPc measured by Pandey et al. in thin films of single carrier devices assuming space-charge-limited current. They found the mobility of Cl-BsubPc to be 4.5×10^{-8} $cm^2\ V^{-1}\ s^{-1}$ for hole transport and 5.2×10^{-10} $cm^2\ V^{-1}\ s^{-1}$ for electron transport.[74]

DEVICE PROPERTIES

To date, Cl-BsubPc has been the prototypical BsubPc incorporated into organic electronic devices. As such this section focuses almost entirely on the body of work on this single BsubPc derivative. Cl-BsubPc was first explored in

organic thin film photovoltaic cells (OPVs) in 2006 by Forrest and Thompson.[37] This exploratory work tested Cl-BsubPc as a new donor molecule with fullerene (C_{60}) as an acceptor in a planar bilayer configuration. Its large band gap and deep frontier orbital energy levels generated a high open circuit voltage (V_{oc}) of 0.97 V resulting in a power conversion efficiency of 2.1% (Figure 6). Device optimization found an optimal thickness for Cl-BsubPc to be 13 nm to obtain the highest device performances with a corresponding C_{60} thickness of 32.5 nm. Later, Gommans et al. found that efficiencies as high as 3.0% could be achieved for 3.3 mm^2 OPVs,[55] which has been consistently reproduced.[32,75,76] Bulk and gradient heterojunction variants of Gommans' OPV have also been shown to have significantly increased short circuit currents (J_{sc}) due to an increased donor/acceptor interfacial area.[77] Different variants on the heterojunction configuration (bulk, gradient zero end point, and gradient nonzero end point) produced varying results, the latter being optimal and producing a power conversion efficiency of 4.2% with high J_{sc} of 11.4 mA/cm^2. An optimal thickness of 64 nm for the Cl-BsubPc:C_{60} layer was found for the heterojunction layer, thicker than the combination of the thicknesses from the optimal planar bilayer device. The ratio of Cl-BsubPc:C_{60} in the gradients was optimal at 1:4. A two donor cascade system has also been explored as even another variant of the Cl-BsubPc/C_{60} device incorporating Cl-BsubPc as an interface layer between CuPc and C_{60}.[78] Here CuPc/Cl-BsubPc/C_{60} devices were fabricated. In this investigation, the thicknesses of CuPc and Cl-BsubPc were varied, with optimal values of 18 and 2 nm respectively. Despite the unique architecture these devices performed worse than the Cl-BsubPc/C_{60} standard due to a low V_{OC} of 0.42 V resulting from the addition of CuPc (1.3% PCE).[78]

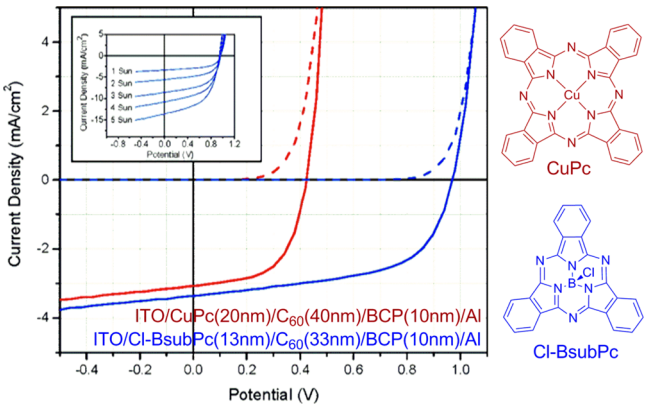

Figure 6. Performance from first Cl-BsubPc/C_{60} device showing high V_{oc} and enhanced performance over CuPc. Figure taken from ref 37 and adapted to include the molecular structure of Cl-BsubPc and CuPc. Reprinted with permission from ref 37. Copyright 2012 American Chemical Society.

A critical parameter for the function of OPVs is the exciton diffusion length within the light absorbing organic material.[79] Three independent investigations on the exciton diffusion lengths in the Cl-BsubPc/C_{60} photovoltaic cell have been performed using two distinctly different approaches: photoluminescence quenching and measured external quantum efficiency. These methods have estimated an exciton diffusion length of 7.7 nm,[80] 8.0 ± 0.3 nm,[81] and 9.5 ± 0.5 nm[75] (respectively) which are in good agreement with the experimentally determined optimal thickness found in the above-mentioned devices (~13 nm balancing exciton diffusion and light absorption). Unfortunately, this diffusion length is low in comparison to other organic semiconductors (for example: 65 nm for pentacene[82] and 100 nm for diindenoperylene[83]) and thus limits the Cl-BsubPc active layer thickness in an OPV. How structural variations of Cl-BsubPc might affect the diffusion length is not currently known.

Electrical contact materials used as OPV electrodes play an important role in the correct energy level alignment for charge injection into its adjacent Cl-BsubPc material, which effects overall device performance. A variety of materials have been used including metal oxides, self-assembled monolayers, polymers and small molecules. Of the metal oxide hole-selective contacts MoO_3[32,76,84] is primarily used with Cl-BsubPc however V_2O_x[85] and AuO[86] have also been tested although they perform worse in Cl-BsubPc/C_{60} photovoltaic cells than MoO_3. In each case, the implementation of metal oxide contact layers into Cl-BsubPc-based devices has resulted in increased performances over their neat control devices (Table 1). The inclusion of an additional contact within an OPV device inherently adds an additional Ohmic resistance to the overall devices, and thus a slight decrease in J_{SC} is expected and observed in each case. The major gains from the inclusion of these interlayers results from their ability to reduce electron leakage currents, and increase the built in potential by modifying the electrode work function. These enhancements reduce the slight 's-kink' observed in the $J-V$ curve for the control devices resulting from a mobility mismatch or a work

Table 1. Summary of the OPV Devices Fabricated with Cl-BsubPc as a Donor Layer[a]

HIL (nm)	donor (nm)	acceptor (nm)	EIL (nm)	V_{oc} (V)	J_{sc} (mA/cm^2)	FF (%)	η (%)	ref
none	Cl-BsubPc (13)	C_{60} (33)	BCP (10)	0.97	3.36	57	2.1	37
none	Cl-BsubPc (13)	C_{60} (33)	BCP (10)	0.92	5.42	61	3.0	55
MoO_x (5)	Cl-BsubPc (10)	C_{60} (33)	BCP (8)	1.10	5.03	53	2.97	76
MoO_x (10)	Cl-BsubPc:C_{60} 1:4 (66) nonzero point gradient		BCP (10)				4.2	77
none	CuPc (18)/Cl-BsubPc (2)	C_{60} (40)	BCP (8)	0.42	5.16	48	1.29	78
MoOx (5)	Cl-BsubPc (14)	F_{16}CuPc (35)	BCP (8)	0.40	2.54	55	0.56	84
MoO_x (5)	Cl-BsubPc (10)	Cl−F_3BsubPc (10)	BCP (8)	1.10	0.83	22	0.19	32
MoO_x (5)	Cl-BsubPc (10)	Cl−F_6BsubPc (10)	BCP (8)	1.22	1.56	43	0.80	32
MoOx (5)	Cl-BsubPc (10)	Cl−Cl_6BsubPc (27)	BCP (8)	1.31	3.53	58	2.68	32
none	Cl-BsubPc (13)	F−F_{12}BsubPc (33)	BCP (10)	0.94	2.1	49	0.96	34
none	Cl-BsubPc (13)	Cl−F_{12}BsubPc (29)	BCP (10)	0.71	2.2	34	0.52	34

[a]The general structure of each device is ITO/HIL/donor/acceptor/EIL/Al.

function misalignment,[87] allowing these devices to attain a high FF and V_{oc}. Metal oxides are reported to have high work functions,[88] their ability to impact hole transport is proposed to be derived from band bending at the interface from the alignment of Cl-BsubPc with gap states formed from oxygen deficiencies within the layer.[76] These interlayers also boast improvements in device longevity and reproducibility for Cl-BsubPc based devices. Although some researchers report high performances without MoO_3, those which do incorporate MoO_3 produce consistently high results, whereas those without lack consistency.

Chemical surface modification of ITO is another approach to modify its work function and its hole collection ability such that it can be optimized for application with Cl-BsubPc. Three chemically modified surfaces have been prepared from phenylsulphonylchloride, 4-chloro-phenylsulphonylchloride and phenoxy-phosphonyldichloride on ITO.[89] The resulting work function of the ITO was modified by this process decreasing from 4.65 eV (for native ITO) to 5.34 eV. Although the study was not performed on an optimal device, improvement was observed when compared to a reference device. Here they found that as the work function of the electrode approached the HOMO level of Cl-BsubPc, devices produced V_{OC} values closer to their maximum theoretical value. For Cl-BsubPc, both 4-chloro-phenylsulphonylchloride and phenoxy-phosphonyldichloride performed comparably and adequately.

Small molecule hole transport materials have also been effective hole collection layers for Cl-BsubPc-based devices. For example, Kulshreshtha and colleagues[90] studied a series of five small molecule hole selective contacts: 2-TNATA, TBBD, NPB, TPD, and TAPC. These materials were evaluated for charge carrier mobility (which ranged from 1×10^{-2} to 1×10^{-5} $cm^2/(V\ s)$) and HOMO energy alignment (ranging from 5.1 to 5.5 eV) with Cl-BsubPc. The highest performance was achieved when the HOMO alignment of the contacts was 0.2 to 0.3 eV below that of Cl-BsubPc presumably due to an elevated built in potential caused by this energy offset. Hole mobility also affected OPV performance indicated by an increased V_{OC} − albeit its impact was minimal. Overall, TBBD was the preferred contact material, with a HOMO of 5.3 eV and a mobility of 2×10^{-2} $cm^2/(V\ s)$. In a few systems, soluble BsubPcs photovoltaic cells have been fabricated using solution casting methods. In this case, the polymer PEDOT:PSS was used as a solution-processed hole selective contact. In each case, these devices performed well, with device efficiencies above 1%; however, reference devices without PEDOT:PSS were not compared.[41]

In terms of electron selective contacts, solely bathocuproine (BCP) and bathophenanthroline (BPhen) have been tested. Both function as a selective contact as well as a protective layer to safeguard the active layers during metal back contact deposition. In cases where devices were fabricated with and without this layer, devices did not function because of pinholes created by the migration of the vacuum deposited metal electrode.[75] Both silver and aluminum metal electrodes have successfully been used in Cl-BsubPc-based devices. One investigation comparing Al and Ag found a small advantage in the Al contact.[37]

When employed as a electron acceptor material, more BsubPc variants other than Cl-BsubPc have been seen in the literature; however, the examples outlined below all still have an axial halogen atom (in other words, are still halo-BsubPcs). A common approach to converting a donor material into an acceptor material is by adding halogens (commonly fluorine) to their molecular structure.[91] To date, the following halogenated derivatives of BsubPc have been synthesized and their application in OPVs reported: Cl−F_3BsubPc, Cl−F_6BsubPc, Cl−F_{12}BsubPc, F−F_{12}BsubPc, and Cl−Cl_6BsubPc. Thus far, peripherally fluorinated derivatives have shown moderate to poor performance as acceptor compounds their performance is also highly dependent on the selection of a companion electron donor. We would note again that the halo-BsubPcs tend to show irreversible oxidation events[19,40,58] and/or reduction events[28,32,92] by cyclic voltammetry. A study by Gomman et al.[34] showed that the fluorinated derivatives functioned best when paired with Cl-BsubPc, Cl-BsubNc, and Cl-AlPc as electron donors. In some cases, BsubPc acceptors have performed comparably to C_{60} when paired with Cl-BsubPc as a donor such as Cl−Cl_6BsubPc (as shown by Sullivan et al.).[32] In comparison to C_{60}, BsubPc acceptors produce a higher V_{OC} because of their large band gap and the narrow offset between the donor and acceptor frontier orbitals (~0.3 eV offset). Similarly a fluorinated fused BsubPc dimer has been incorporated as an acceptor in OPVs with Cl-BsubPc as a donor producing high power conversion efficiencies of 4% despite a narrow 0.2 eV $HOMO_D$-$HOMO_A$ offset.[93] Although Cl-BsubPc is commonly known as an electron donor material, a recently report highlights its potential as a bipolar material. Beaumont et al. recently reported the use of Cl-BsubPc as an electron acceptor in an organic photovoltaic when paired with tetracene as an electron donor.[33] These devices produced a high V_{OC} (1.24 V) and a power conversion efficiency of 2.9%, outperforming the comparable tetracene/C_{60} device.

Most organic electronic devices utilize contact layers to block excitons from migrating to the electrodes. A unique application of Cl-BsubPc is its use as an exciton blocking selective layer and as a hole transport layer in OLEDs. Chen et al. have shown that Cl-BsubPc inserted as a hole selective contact between ITO and NPB in OLEDs increases the OLED performance.[62] Using XPS and UPS analysis of the deposited films, Chen et al. hypothesized that Cl-BsubPc undergoes a chemical change when in contact with NPB by abstraction of the chlorine atom forming cationic $BsubPc^+$ and a $[Cl^-][NPB]$ complex. They further hypothesized that these charged species form gap states in the BsubPc material which is proposed to greatly increase charge injection. It should be pointed out that the formation of such a complex or the abstraction of the chloride from Cl-BsubPc by NPB has not been observed elsewhere, nor does it seem to be based on a known chemical reaction. However, the presence of gap states is likely and this observation was later exploited by utilizing Cl-BsubPc as a molecular dopant in NPB layers for OLEDs.[94] In this example, charge injection was once again increased because of the generated gap states. Optimal performance was found at low doping concentrations of 5%. More recently, Chen et al. explored the use of Cl-BsubPc in the commonly used LiF electron selective contact.[95] Here once again they discovered an improvement in charge injection associated with the generation of gap states arising from the abstraction of the chlorine atom in Cl-BsubPc resulting from lithium release from LiF.

BsubPcs also function in organic thin film transistors. Although there is a general paucity of BsubPc transistor literature, one example exists utilizing Cl-BsubPc as the semiconductor layer.[35] In this study, Cl-BsubPc was deposited on an insulating polymer, then either gold or calcium contacts were deposited in order to operate the devices. The researchers

Scheme 1. Synthetically Accessible Axial Derivatives of BsubPcs Derived from halo-BsubPcs and pseudohalo-BsubPcs; R = alkyl or aryl

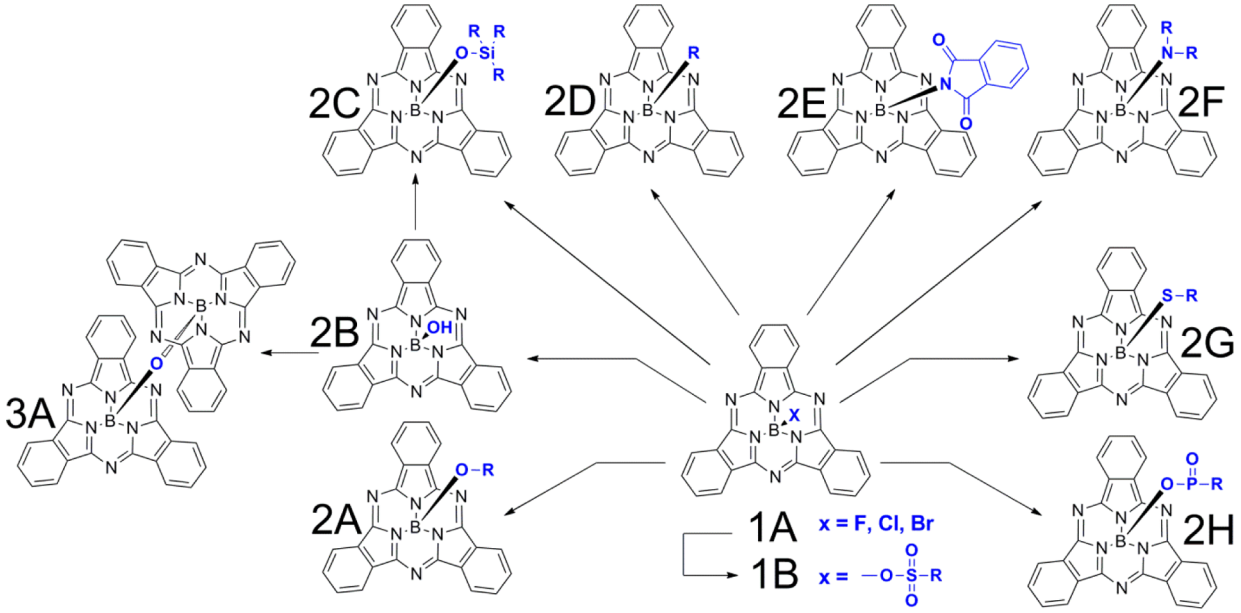

discovered that Cl-BsubPc behaved as an electron transport material when operated in a nitrogen environment with a mobility of 5.4×10^{-5} $cm^2/(V\ s)$; however, in air, Cl-BsubPc switched to favor hole transport, demonstrating that the presence of oxygen in BsubPc films can change charge transport behavior. This type of behavior is also observed for phthalocyanines,[96] suggesting that encapsulation technology would be required for long-term device testing or commercial application when Cl-BsubPc is employed in the device.

BEYOND Cl-BsubPc AND AXIAL HALIDES

From the highlights above it is evident that the majority of the study of BsubPcs in organic electronic devices has been carried out using halo-BsubPcs and mostly the prototypical Cl-BsubPc. Given the advances made in the chemistry of BsubPcs by Kobyashi,[97] Torres,[15,69,98,99] and others, including recently our group,[13,18,22−24,45,60,66,71,72,100] it is therefore surprising that the field has not moved beyond Cl-BsubPc to the more widespread use of other BsubPc derivatives.

We begin by examining the synthetic methods available for BsubPcs. Currently, BsubPcs are synthesized in two steps, first by formation of the BsubPc macrocycle via condensation of phthalonitriles in the presence of a boron trihalide forming a halo-BsubPc (X-BsubPc, where X = fluoro, chloro, or bromo). Subsequent displacement of the halide with a nucleophile leads to BsubPc with additional functionalization. The two-step chemistry provides for two opportunities to introduce structural variation into the BsubPc molecule first fixing the physiochemical character of the periphery in place then adding further functionality or fine-tuning of its properties through introduction of an alternative axial fragment to a halide. The peripheral derivation of BsubPcs through the chemical modification of the phthalonitrile is known from phthalocyanine chemistry.[7] Many methods to produce BsubPc derivatives have been developed and have been previously reviewed.[15,101] Briefly, their synthesis involves the condensation of phthalonitrile dissolved in an organic solvent at elevated temperatures in the presence of a boron trihalide which templates the formation of BsubPc of which boron trifluoride,[10,102] boron trichloride,[10,102,103] and boron tribromide[10,102] have all been used. Halogen exchange between axial halogens can also be performed. Conversion of Cl-BsubPc to F-BsubPc can be performed using boron trifluoride diethyletherate[61] or silver tetrafluoroborate.[104] Conversion from Br-BsubPc to Cl-BsubPc can be facilitated by aluminum chloride.[60]

More recently, pseudohalide-BsubPcs have been explored as precursors to more complex BsubPcs. The first example was the triflate of BsubPc (TfO-BsubPc) synthesized by Torres and colleagues.[104] The procedure involves reaction of Cl-BsubPc in dry toluene with 1.25 equiv of silver triflate (at 40 °C, 1−2 h) or trimethylsilyl trifluoromethanesulfonate (at reflux, >4 h). Concurrent with the disclosure by Torres et al., our group reported the synthesis and isolation of a series of pseudohalide-BsubPcs including the mesylate, tosylate, benzylate, chlosylate, and nosylate of BsubPc (MsO-BsubPc, TsO-BsubPc, BzO-BsubPc, ClsO-BsubPc, and NsO-BsubPc, respectively; BzO, phenylsulfonate; ClsO, 4-chlorophenylsulfonate; NsO, 3-nitrophenylsulfonate). Each could also be used as precursors to other BsubPcs, although each reacts with a different rate.[71]

The axial derivation of halo-BsubPcs is being continually being expanded upon.[60,68,99,104] Nucleophiles such as phenols,[28,99] bisphenols,[18,30] alcohols,[28] hydroxyl,[69,70,102,105] alkynylmagnesium bromides,[68,106] phthalimides,[23] phosphates, and phosphonates[107,108] have been shown to react with halo-BsubPcs forming their respective axial derivatives. Other nucleophiles such as silanols, anilines, thiols, and thiophenols can also be used by activating the boron−halogen bond[60] or by utilizing alternative BsubPc starting materials such as HO-BsubPc[69] or TfO-BsubPc.[104] See Scheme 1, in which each of these derivatives has been categorized for later reference.

Oxygen bearing nucleophiles (category 2A, Scheme 1) such as phenols, bisphenols, and alcohols have been frequently used to add chemical functionality to BsubPcs due to the plethora of commercially available derivatives and ease of synthesis. Their reaction typically involves the condensation with halo-BsubPcs (or pseudohalogens) to form their respective BsubPc at reflux

dx.doi.org/10.1021/am3015197 | ACS Appl. Mater. Interfaces 2012, 4, 5055−5068

in toluene, chlorobenzene, dichlorobenzene, chloronaphthalene, or other aromatic solvents over prolonged periods of time.[18,30,99] This reaction is believed to be S_N1 in nature[15] supported by the isolation and characterization of a positive boron cation of BsubPc by Reed and co-workers.[109] Often, and likely due to the challenges of keeping a reaction anhydrous for long periods of time, HO-BsubPc is seen as a byproduct (from hydrolysis of the halo-BsubPc) or its self-condensation product μ-oxo-$(BsubPc)_2$. μ-Oxo-$(BsubPc)_2$ can be easily identified in a reaction mixture because of its unique absorption spectrum, which is different from other BsubPc derivatives.[69] Our group has recently shown that the reaction of halo-BsubPcs with phenols can be activated using $AlCl_3$. Once activated, the reaction proceeds at low temperatures (<60 °C or even room temperature) in a variety of solvents within 1−2 h.[60] Although the presence of water under these conditions can produce HO-BsubPc, the exclusion of water over these short time periods is facile. HO-BsubPc is, however, more challenging to obtain in high yields (category 2B), requiring the use of KOH, sulphuric acid or water in a mixture of polar and nonpolar solvents in order to to codissolve water and the halo-BsubPc.[69,102,105] Often, during the formation of HO-BsubPc, μ-oxo-$(BsubPc)_2$ is formed through self-condensation (category 3A).[69] HO-BsubPc has also been shown to be an effective precursor to the synthesis of trialkylsiloxy-BsubPcs (category 2C);[69,70] however, they can also be synthesized from X-BsubPc and TfO-BsubPc.[103,104]

The axial attachment of carbon through carbon-based nucleophiles (category 2D, Scheme 1) can be performed using Grignard reagents including Grignards of alkynyls,[68] linear or branched alkyls, and aryls.[104] In the synthesis of ethynylaryl-BsubPcs, 1 equiv of Cl-BsubPc (1A, Scheme 1) and 2 equiv of the ethynylaryl Grignard are combined at 60 °C in anhydrous THF. The reaction requires 1−24 h, depending on nature of the ethynylaryl and produces yields typically between 22 and 74%. No assumption has been made regarding the mechanism of this reaction. Aryl or alkyl derivatives can be similarly accessed starting from triflate-BsubPc (1B, Scheme 1) by adding the Grignard reagent (2 equiv) in dry toluene and 1.25 equiv of diisopropylethylamine at 40 °C for 6 h, with yields between 55 and 68%.[104] Carbon only axial substituents can also be formed during the BsubPc macrocycle formation by using an alkyl and an aryl boron (for example phenyldichloroborane) in place of a boron halide. Yields are, however, typically much lower using this methodology.[69,110]

Nitrogen nucleophiles do not undergo simple reaction with halo-BsubPcs with the exception of phthalimides (category 2E),[23] which require long reaction times (4 days) at elevated temperatures (refluxing dichlorobenzene). However, nitrogen-based nucleophiles (category 2f) do react with TfO-BsubPc[104] or with Cl-BsubPc when activated with $AlCl_3$[60] to produce their respective BsubPc derivatives. In the case of $AlCl_3$ activation, reaction conditions are mild (60 °C, 8 h).

Sulfur-based nucleophiles (category 2G) have also been consistently unattainable by direct reaction of a sulfur nucleophile with a halo-BsubPc. However, the same two methods (TfO-BsubPc[104] and $AlCl_3$ activation[43]) that work for nitrogen nucleophiles have worked with thiophenols,[43] and thiolalkyls.[104]

Phosphorus-based nucleophiles (category 2H) have also recently been used to access phosphinoxy-BsubPcs. They were first described in a patent,[107] and recently in the scientific literature.[107,108] The reaction of 2 equiv of a selected phosphinic acid with Cl-BsubPc in dichlorobenzene at reflux for 5 h was sufficient to produce the desired derivatives with yields ranging between 67 and 19%.

MATERIAL PROPERTIES AND DEVICE PERFORMANCE

Though some axial derivatives of BsubPcs exist, a strong understanding of how these modifications affect performance in organic electronic devices remains largely unknown. The application of PhO-BsubPcs, Phth-BsubPcs,[23] and arylethynyl-BsubPcs[68,106] have been reported with the former having been largely developed by our laboratories at the University of Toronto. Similar to the halo-BsubPcs, it is important to understand their structure property relationships as they pertain to both photophysical and electrophysical properties, including those same while in an organic electronic device. In this section, we highlight our work on PhO-BsubPcs and Phth-BsubPcs and specifically outline the effect (or lack thereof) of axial substitution on the frontier orbital energy levels, band gap, sublimability or solubility, charge transport properties, and organic electronics device performance.

Prior to device fabrication, we must first consider how axial substitution of a BsubPc affects the frontier molecular energy levels of PhO-BsubPcs. In a recent paper, we created an experimentally validated model to predict frontier molecular orbital variation based on the molecular structure of PhO-BsubPcs.[13] We began by constructing 106 different PhO-BsubPc derivatives *in silico*, all of which in principle were synthetically accessible. After modeling at both the semi-empirical and DFT levels, we synthesized seven different PhO-BsubPcs having various substituents whereby the *in silico* modeling predicted the seven would span a range of HOMO and LUMO energy levels. We then determined the positions of the frontier orbitals (and consequently their band gaps) using a mixture of cyclic voltametry (CV), ultraviolet photoemission spectroscopy (UPS), and UV−visible spectroscopy. The results were that for PhO-BsubPcs, the relative position within the molecule of the frontier orbitals had a minimal response to variations at both the peripheral and axial positions (Figure 7),[13] whereas the energy levels of the HOMO and LUMO were six times more sensitive to substitution on the peripheral positions of the BsubPc as compared to substitution at the axial position. At the extremes of the range were 3,4-diMe-PhO-

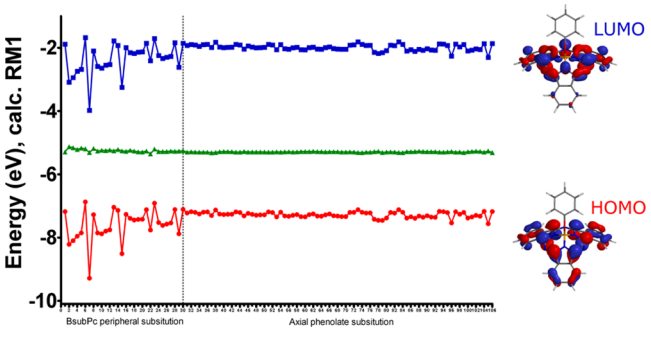

Figure 7. Predicted HOMO (red) and LUMO (blue) molecular orbital energy levels and the band gap (green) for a series of axial and peripheral substituted derivatives of phenoxy-BsubPc. The green triangles indicates the band gap. Figure taken from ref 13 and adapted to include a visualization of the orbital distributions generally observed for phenoxy-BsubPc. Reprinted with permission from ref 13. Copyright 2012 American Chemical Society.

dx.doi.org/10.1021/am3015197 | ACS Appl. Mater. Interfaces 2012, 4, 5055−5068

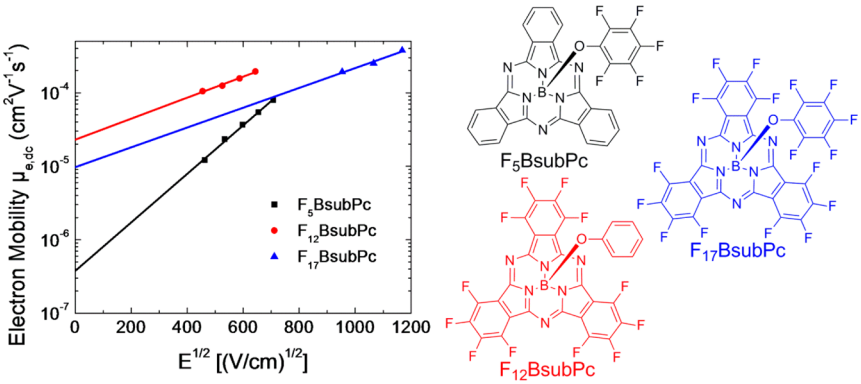

Figure 8. Field-dependent mobility at 300 K of F_5BsubPc (black), F_{12}BsubPc (red) and F_{17}BsubPc (blue) (molecular structures shown). Solid lines are best fits for the data and show the extrapolation back to obtain zero field mobility. Adapted from figure in ref 45. Reprinted with permission from 45. Copyright 2012 American Chemical Society.

BsubPc and F_{17}BsubPc, spanning a HOMO range from 5.42 to 6.65 eV and a LUMO range from 3.28 to 4.54 eV. Thus the HOMO and LUMO energy levels can be varied over a relatively large range of >1 eV. The majority of the changes in the energy levels are attributable to peripheral substituents.

We have also estimated the frontier orbital energies of Phth-BsubPcs using CV. As for Phth-BsubPcs, we have found that substitution on the phthalimide axial position with perchlorination changes its frontier energy levels by less than 0.1 eV.[23] Substitution on the axis of arlyethynyl-BsubPcs similarly showed little change in frontier orbitals, effecting their electrochemical redox half-waves by >0.1 V.[68]

We have also studied how axial substitution of BsubPcs affects their solubility. In the first paper of a series, we compared Cl-BsubPc, two PhO-BsubPcs, and seven dimeric bisphenoxy-$(BsubPc)_2$s. We observed that the solubility of the dimers and PhO-BsubPcs were on average 1 and 2 orders of magnitude higher than the solubility of Cl-BsubPc (respectively). This led us to the conclusion that Cl-BsubPc is more pigment-like (using terms borrowed from colorant chemistry), as are normal phthalocyanines. Thus we set out to established methods for producing highly soluble BsubPcs. One of the more common methods used in organic electronic materials to impart solubility is to introduce long chain alkyl (or branched alkyl) molecular fragments into the molecule. Interaction of the large hydrocarbons with solvent molecules thus imparts the solubility. Indeed, this approach works with BsubPcs, 3-pentadecylphenoxy-BsubPc has a solubility of $>1 \times 10^{-2}$ M in most common solvents.[66] Diaz and colleagues showed 4-*tert*-butylphenoxy-BsubPc is also very soluble.[111] Although the exact solubility was not determined, they were able to successfully dissolve these compounds and deposit them from solution as thin films in OLED devices. More recently, we have shown that the more atom economical derivatives 3-methylphenoxy-BsubPc and 3,4-dimethylphenoxy-BsubPc are also highly soluble ($>1 \times 10^{-2}$ M).[101] Peripheral modified BsubPcs can also be used to impart solubility;[66] however, using such an approach changes both the symmetry of the BsubPc as well as its physical and chemical properties (recalling the discussion above regarding sensitivity to peripheral substitution[10]). Approaches to creating water-soluble BsubPcs also exist and generally involve the formation of a water-soluble salt.[112]

Sublimability is also of concern. BsubPc derivatives with axial fluoro-, chloro-, methoxy-, and methyl- subsituents, and derivatives containing dodecafluoro and hexachloro peripheral substitutents have been reported as sublimable.[13,24,32,34,37] We have also shown that Phth-BsubPcs derivatives are stable under sublimation conditions.[23] The stability of arylethynyl-BsubPcs under sublimation conditions is unknown. We have shown that fluorination can be used as a strategy to reduce the sublimation temperature of PhO-BsuPcs.[24]

We have also studied the basic electron mobilities of a series of BsubPc derivatives we refer to as F_5BsubPc, F_{12}BsubPc, and F_{17}BsubPc using admittance spectroscopy (Figure 8).[45] Their electron mobilities were found to be field-dependent, following a Poole-Frenkel type relation with zero field mobilities of 4×10^{-7}, 2×10^{-5}, and 1×10^{-5} cm^2 V^{-1} s^{-1}, respectively. Electron mobilities of $\sim 1 \times 10^{-4}$ cm^2 V^{-1} s^{-1} were determined at field strengths typical for some organic electronic devices. In each case the electron mobility is notably higher than that of Cl-BsubPc. We also found the electric field dependence of mobility was found to correlate to their solid-state arrangement as determined by X-ray crystallography.

Axial derivatives of BsubPcs have been applied in OLEDs. Díaz et al. has described the synthesis of five soluble PhO-BsubPc derivatives and their application as electrolumiphores (emitters) in solution deposited/fabricated OLEDs.[111] These devices incorporated the BsubPc derivative as a dopant (less than 20% by weight) in a polyspirofluorene−arylamine copolymer and produced OLEDs with a narrow electroluminescence (60−90 nm width at half of its maximum intensity) a high turn on voltage of 10 V, low stability and moderate current efficiencies of 0.1 cd/A (100 cd/m^2). The first vacuum fabricated OLEDs incorporating BsubPcs as emitters were constructed in our laboratories at the University of Toronto. The same series of fluorinated PhO-BsubPcs were used (F_5BsubPc, F_{12}BsubPc and F_{17}BsubPc).[24] We demonstrated that BsubPcs can be used as either or both electron transporters and emitters. OLEDs had low turn on voltages of 3.4 V when appropriate electron selective contacts were selected. In this case TPBi in place of the more commonly used LiF was desirable. F_5BsubPc performed best with a maximum current efficiency of 0.03 cd/A (122 cd/m^2) and an incredibly narrow 31 nm width at half of its maximum intensity. Interested in further enhancing performance, we later incorporated F_5BsubPc as a dopant emitter in a variety of host materials. As a dopant, F_5BsubPc produced record current efficiencies of 1.5 cd/A for a BsubPc derivative, and improved color purity (Figure 9).[22]

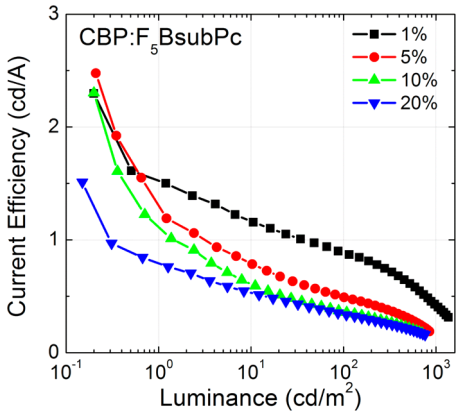

Figure 9. Current efficiency as a function of luminance for OLED devices with F_5BsubPc doped in CBP at 1 to 20 wt %. The device structure used was ITO/MoO3(1 nm)/CBP(45 nm)/CBP:F5BsubPc-(15 nm)/TPBi(30 nm)/LiF(1 nm)/Al(100 nm). Adapted with permission from ref 22. Copyright 2012 American Chemical Society.

As mentioned above, we also reported the synthesis of a new class of BsubPc made by using phthalimides as nucleophiles – the Phth-BsubPcs. We found Phth-BsubPcs to be electrochemically bipolar.[23] Planar bilayer OLEDs with Phth-BsubPcs incorporated into the devices as either a hole-transporter/emitter or an electron-transporter/emitter were fabricated. In either configuration the resulting OLEDs produced comparable maximum current efficiencies: 0.03 cd/A (143 cd/m^2) as electron transport emitters and 0.02 cd/A (77 cd/m^2) as hole transport emitters thus demonstrating the bipolar electrochemical behavior translated well in the solid state of an OLED. Although no record OLED efficiencies were achieved with these unoptimized devices, the results do support the conclusion that BsubPcs are a promising class of orange emitters with a remarkably narrow emission width and excellent electrical performance in OLEDs.

As noted above, the vast majority of publications on the application of BsubPcs in OPVs are limited to Cl-BsubPc. There are, however, three cases reported where other BsubPc derivatives have been used in OPVs as donor materials (see Table 2). Two cases utilized solution processable (soluble) derivatives namely 2-allylphenoxy-BsubPc,[41] and a series of four axially attached thiophene-BsubPcs.[31] Interestingly, both cases produced devices with relatively high performance as indicated by power conversion efficiencies >1%. The devices in each case were fabricated with a PEDOT:PSS layer as a hole selective contact overcoated with a series of vacuum deposited layers comprising C_{60}/BCP/Al as the acceptor, the electron selective contact and the top electrode respectively. For the thiophene-BsubPcs, the type of axial attachment used (alkynyl or phenoxy) had less of an impact on performance than then length of the thiophene chain itself (2 or 4 units where studied). Derivatives with the shorter chain length performed best because of their more conformal and amorphous film behavior. These devices each displayed a higher J_{SC} relative to Cl-BsubPc, but a lower V_{OC} and FF.

Very recently, we have evaluated F_5BsubPc in OPVs (Table 2).[113] Here the compound was deposited by sublimation, unlike the previous examples. This material displayed both electron-donor and electron-acceptor behavior in separate device configurations when paired with C_{60} or Cl-BsubPc and pentacene respectively. In each device configuration V_{OC} of >1 V and power conversion efficiencies >1% were achieved with unoptimized devices (Figure 10). Analysis of the interfaces in these devices by UPS found that the Cl-BsubPc/F_5BsubPc heterojunctions had small (ca. 0.1 eV) offsets in both HOMO and LUMO energies but good rectification and photovoltaic activity could still be achieved. The F_5BsubPc/C_{60} heterojunction was more conventional with a 0.7 eV HOMO offset while also producing good rectification and photovoltaic activity. Incident and absorbed photon power conversion efficiencies demonstrated the presence of a charge transfer complex between F_5BsubPc and C_{60} or Cl-BsubPc. We found that these specific interactions contribute significantly to the performance in these devices. With its electron donor or acceptor capabilities, strong light absorption, sublimability and high open circuit voltages in OPVs, F_5BsubPc highlights that

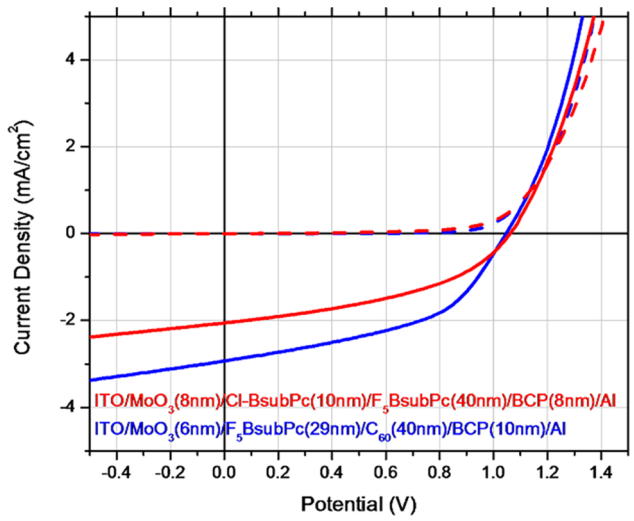

Figure 10. Current density versus electric potential average performance plot of OPV devices fabricated with F_5BsubPc as either an acceptor (red) or a donor material (blue).

Table 2. Summary of All Axially Modified BsubPcs in OPV Devices[a]

HIL (nm)	donor (nm)	acceptor (nm)	EIL (nm)	V_{oc} (V)	J_{sc} (mA/cm^2)	FF (%)	η (%)	ref
PEDOT:PSS	A-BsubPc (20)	C_{60} (32)	BCP (10)	0.74	5.03	46	1.71	41
PEDOT:PSS	2Tp-SubPc	C_{60} (32)	BCP (10)	0.73	3.72	51	1.39	
PEDOT:PSS	2Ta-SubPc	C_{60} (32)	BCP (10)	0.70	3.90	50	1.39	
PEDOT:PSS	4Tp-SubPc	C_{60} (32)	BCP (10)	0.63	3.30	34	0.70	
PEDOT:PSS	4Ta-SubPc	C_{60} (32)	BCP (10)	0.57	4.05	45	1.04	
MoO_3 (6)	F_5BsubPc (29)	C_{60} (40)	BCP (10)	1.05	2.96	48	1.49	113
MoO_3 (8)	Cl-BsubPc (10)	F_5BsubPc (40)	BCP (8)	1.06	2.06	43	0.94	113

[a]The general structure for each device in this table is ITO/HIL/donor/acceptor/EIL/Al or Ag.

dx.doi.org/10.1021/am3015197 | ACS Appl. Mater. Interfaces 2012, 4, 5055−5068

axial derivatives other than halides of BsubPcs if properly designed can at the very least have competitive performance to Cl-BsubPc in devices made by vacuum deposition.

CLOSING REMARKS/CONCLUSIONS

Thus far, BsubPcs have made remarkable progress since their discovery in 1972 and their first use as an organic semiconductor in 2006. As an organic semiconductor it possesses many desirable properties: an intense and narrow (~30 nm) orange fluorescence, an intense and narrow absorbance (ε = 50 000−80 000 M^{-1} cm^{-1}), conformal yet crystalline thin films, low sublimation temperatures, tunable solubility, tunable electronic properties, and in some cases bipolar electrochemistry and charge transport.

In our opinion, the following areas need addressing in order to progress BsubPcs as a high performance class of organic semiconductors. Cl-BsubPc has made significant progress as a high performance material for OPVs however the axial chlorine does not present an obvious advantage in these devices - similar success could be found for other axial derivatives (for example, F_5BsubPc). Future efforts with axial substituted materials should be undertaken to explore the large degree of chemical variability available at that position and the potential to tune the properties of the BsubPc for application in organic electronic devices. A strong understanding of the relationship between mobility and the solid state arrangement of BsubPcs needs to be developed in order to aid in their molecular design and crystal engineering to improve device performance beyond current benchmarks, for example, to achieve higher charge carrier mobilities. The inherent bipolar electrochemical stability of some BsubPc derivatives is rare and should be taken advantage of in device application. In addition, a greater understanding of the design principles required to create bipolar BsubPc materials should be developed. BsubPc materials seem to be highly selective to interfaces, forming functional heterojunctions when paired with some organic semiconductors and not functioning with others. The cone shape structure of these materials makes interpreting their interfacial behavior challenging. So, finally, the interfacial templation/alignment of BsubPc on different surfaces relevant to organic electronics should be explored to understand how material selection impacts device performance.

AUTHOR INFORMATION

Corresponding Author

*E-mail: tim.bender@utoronto.ca.

Notes

The authors declare no competing financial interest.

REFERENCES

(1) Gill, W. *J. Appl. Phys.* **1972**, *43* (12), 5033−5040.
(2) Mott, S. N. F.; Gurney, R. W. *Electronic Processes in Ionic Crystals*; Oxford University Press: Oxford, U.K., 1940.
(3) Helfrich, W.; Schneide, W. *Phys. Rev. Lett.* **1965**, *14* (7), 229−&.
(4) Albery, W. J.; Archer, M. D. *Nature* **1977**, *270* (5636), 399−402.
(5) Tang, C. W. *Appl. Phys. Lett.* **1986**, *48* (2), 183−185.
(6) Tang, C. W.; Vanslyke, S. A. *Appl. Phys. Lett.* **1987**, *51* (12), 913−915.
(7) McKeown, N. B., *Phthalocyanine Materials: Synthesis, Structure and Function*; Cambridge University Press: Cambridge, U.K., 1998.
(8) Brumbach, M.; Placencia, D.; Armstrong, N. R. *J Phys Chem C* **2008**, *112* (8), 3142−3151.
(9) Marks, T. J.; Stojakovic, D. R. *J. Am. Chem. Soc.* **1978**, *100* (6), 1695−1705.
(10) Meller, A.; Ossko, A. *Monatsh. Chem.* **1972**, *103* (1), 150−155.
(11) Zdravkovski, D.; Milletti, M. C. *J. Mol. Struct. Theochem* **2005**, *717* (1−3), 85−89.
(12) Gonzalez-Rodriguez, D.; Torres, T.; Guldi, D. M.; Rivera, J.; Herranz, M. A.; Echegoyen, L. *J. Am. Chem. Soc.* **2004**, *126* (20), 6301−13.
(13) Morse, G. E.; Helander, M. G.; Stanwick, J.; Sauks, J. M.; Paton, A. S.; Lu, Z. H.; Bender, T. P. *J. Phys. Chem. C* **2011**, *115* (23), 11709−11718.
(14) González Rodríguez, D.; Torres, T. *Eur. J. Org. Chem.* **2009**, *2009* (12), 1871−1879.
(15) Claessens, C. G.; González-Rodríguez, D.; Torres, T. *Chem. Rev.* **2002**, *102* (3), 835−854.
(16) Claessens, C. G.; Torres, T. *Tetrahedron Lett.* **2000**, *41* (33), 6361−6365.
(17) Ferguson, L. N. *Chem. Rev.* **1948**, *43* (3), 385−446. Lewis, G. N.; Calvin, M. *Chem. Rev.* **1939**, *25* (2), 273−328.
(18) Morse, G. E.; Paton, A. S.; Lough, A.; Bender, T. P. *Dalton Trans.* **2010**, *39* (16), 3915−22.
(19) Kipp, R. A.; Simon, J. A.; Beggs, M.; Ensley, H. E.; Schmehl, R. H. *J. Phys. Chem. A* **1998**, *102* (28), 5659−5664.
(20) Martín, G.; Rojo, G.; Agulló-López, F.; Ferro, V. R.; García de la Vega, J. M.; Martínez-Díaz, M. V.; Torres, T.; Ledoux, I.; Zyss, J. *J. Phys. Chem. B* **2002**, *106* (51), 13139−13145.
(21) Reichardt, C. *Chem. Rev.* **1994**, *94* (8), 2319−2358.
(22) Helander, M. G.; Morse, G. E.; Qiu, J.; Castrucci, J. S.; Bender, T. P.; Lu, Z. H. *ACS Appl. Mater. Interfaces* **2010**, *2* (11), 3147−52.
(23) Morse, G. E.; Castrucci, J. S.; Helander, M. G.; Lu, Z. H.; Bender, T. P. *ACS Appl. Mater. Interfaces* **2011**, *3* (9), 3538−44.
(24) Morse, G. E.; Helander, M. G.; Maka, J. F.; Lu, Z. H.; Bender, T. P. *ACS Appl. Mater. Interfaces* **2010**, *2* (7), 1934−1944.
(25) Mertz, E. L.; Tikhomirov, V. A.; Krishtalik, L. I. *J. Phys. Chem. A* **1997**, *101* (19), 3433−3442.
(26) Ferro, V.; Garcia de la Vega, J.; Gonzalez-Jonte, R.; Poveda, L. *J. Mol. Struct. Theochem* **2001**, *537* (1−3), 223−234.
(27) Rio, Y.; Rodriguez-Morgade, M.; Torres, T. *Org. Biomol. Chem.* **2008**, *6* (11), 1877−94.
(28) Kasuga, K.; Idehara, T.; Handa, M.; Ueda, Y.; Fujiwara, T.; Isa, K. *Bull. Chem. Soc. Jpn.* **1996**, *69* (9), 2559−2563.
(29) Ferro, V. R.; De La Vega, J. M. G.; Claessens, C. G.; Poveda, L. A.; Gonzalez-Jonte, R. H. *J. Porphyr. Phthalocyan.* **2001**, *5* (6), 491−499.
(30) Fukuda, T.; Olmstead, M. M.; Durfee, W. S.; Kobayashi, N. *Chem. Commun.* **2003**, *11*, 1256−7.
(31) Mauldin, C. E.; Piliego, C.; Poulsen, D.; Unruh, D. A.; Woo, C.; Ma, B.; Mynar, J. L.; Fréchet, J. M. J. *ACS Appl. Mater. Interfaces* **2010**, *2* (10), 2833−2838.
(32) Sullivan, P.; Duraud, A.; Hancox, I.; Beaumont, N.; Mirri, G.; Tucker, J. H. R.; Hatton, R. A.; Shipman, M.; Jones, T. S. *Adv. Energy Mater.* **2011**, *1* (3), 352−355.
(33) Beaumont, N.; Cho, S. W.; Sullivan, P.; Newby, D.; Smith, K. E.; Jones, T. S. *Adv. Funct. Mater.* **2012**, *22*, 561.
(34) Gommans, H.; Aernouts, T.; Verreet, B.; Heremans, P.; Medina, A.; Claessens, C. G.; Torres, T. *Adv. Funct. Mater.* **2009**, *19* (21), 3435−3439.
(35) Yasuda, T.; Tsutsui, T. *Mol. Cryst. Liq. Cryst.* **2006**, *462* (1), 3−9.
(36) Cho, S. W.; Piper, L. F. J.; DeMasi, A.; Preston, A. R. H.; Smith, K. E.; Chauhan, K. V.; Sullivan, P.; Hatton, R. A.; Jones, T. S. *J. Phys. Chem. C* **2010**, *114* (4), 1928−1933.
(37) Mutolo, K. L.; Mayo, E. I.; Rand, B. P.; Forrest, S. R.; Thompson, M. E. *J. Am. Chem. Soc.* **2006**, *128* (25), 8108−9.
(38) Fulford, M. D., J.; Paton, A. S.; Morse, G. E.; Brisson, E.; Lough, A. J.; Bender, T. P. *J. Chem. Eng. Data* **2012**, in press.
(39) del Rey, B.; Keller, U.; Torres, T.; Rojo, G.; Agulló-López, F.; Nonell, S.; Martí, C.; Brasselet, S.; Ledoux, I.; Zyss, J. *J. Am. Chem. Soc.* **1998**, *120* (49), 12808−12817.
(40) Iglesias, R. S.; Claessens, C. G.; Rahman, G.; Herranz, M.; Guldi, D. M.; Torres, T. *Tetrahedron* **2007**, *63* (50), 12396−12404.

(41) Ma, B.; Miyamoto, Y.; Woo, C. H.; Fréchet, J. M. J.; Zhang, F.; Liu, Y. *Proc. of SPIE* **2009**, *7416*, 74161E.
(42) Das, B.; Tokunaga, E.; Shibata, N.; Kobayashi, N. *J. Fluorine Chem.* **2010**, *131* (5), 652−654.
(43) Lee, S.; Suh, H. *Bull. Korean Chem. Soc.* **1999**, *20*, 991−992.
(44) Chen, Z.; Xia, C.; Wu, Y.; Zuo, X.; Song, Y. *Inorg. Chem. Commun.* **2006**, *9* (2), 187−191.
(45) Castrucci, J. S.; Helander, M. G.; Morse, G. E.; Lu, Z.-H.; Yip, C. M.; Bender, T. P. *Cryst. Growth Des.* **2012**, *12* (3), 1095−1100.
(46) Chauhan, K. V.; Sullivan, P.; Yang, J. L.; Jones, T. S. *J Phys Chem C* **2010**, *114* (7), 3304−3308.
(47) Mannsfeld, S.; Relchhard, H.; Fritz, T. *Surf. Sci.* **2003**, *525* (1−3), 215−221.
(48) Yanagi, H.; Schlettwein, D.; Nakayama, H.; Nishino, T. *Phys. Rev. B* **2000**, *61* (3), 1959.
(49) Yanagi, H.; Ikuta, K.; Mukai, H.; Shibutani, T. *Nano Lett.* **2002**, *2* (9), 951−955.
(50) Berner, S.; Brunner, M.; Ramoino, L.; Suzuki, H.; Guntherodt, H. J.; Jung, T. A. *Chem. Phys. Lett.* **2001**, *348* (3−4), 175−181.
(51) Berner, S.; De Wild, M.; Ramoino, L.; Ivan, S.; Baratoff, A.; Güntherodt, H. J.; Suzuki, H.; Schlettwein, D.; Jung, T. *Phys. Rev. B* **2003**, *68* (11), 115410.
(52) Petrauskas, V.; Lapinskas, S.; Tornau, E. E. *J. Chem. Phys.* **2004**, *120* (24), 11815−21.
(53) Jiang, N.; Wang, Y.; Liu, Q.; Zhang, Y.; Deng, Z.; Ernst, K. H.; Gao, H. J. *Phys. Chem. Chem. Phys.* **2010**, *12* (6), 1318−22.
(54) Yanagi, H.; Ikuta, K. *Surf. Sci.* **2005**, *581* (1), 9−16.
(55) Gommans, H.; Cheyns, D.; Aernouts, T.; Girotto, C.; Poortmans, J.; Heremans, P. *Adv. Funct. Mater.* **2007**, *17* (15), 2653−2658.
(56) Kim, J.; Yim, S. *Appl. Phys. Lett.* **2011**, *99* (19), 193303.
(57) Horowitz, G.; Hajlaoui, M. E. *Adv. Mater.* **2000**, *12* (14), 1046−1050.
(58) Ros-Lis, J. V.; Martinez-Manez, R.; Soto, J. *Chem. Commun.* **2005**, *42*, 5260−5262.
(59) Palomares, E.; Martinez-Diaz, M. V.; Torres, T.; Coronado, E. *Adv. Funct. Mater.* **2006**, *16* (9), 1166−1170.
(60) Morse, G. E.; Bender, T. P. *Inorg. Chem.* **2012**.
(61) Rodriguez-Morgade, M. S.; Claessens, C. G.; Medina, A.; Gonzalez-Rodriguez, D.; Gutierrez-Puebla, E.; Monge, A.; Alkorta, I.; Elguero, J.; Torres, T. *Chemistry* **2008**, *14* (4), 1342−50.
(62) Chen, Y. H.; Chang, J. H.; Lee, G. R.; Wu, I. W.; Fang, J. H.; Wu, C. I.; Pi, T. W. *Appl. Phys. Lett.* **2009**, *95* (13), 133302.
(63) Claessens, C. G.; Torres, T. *Chem. Commun.* **2004**, *11*, 1298−9.
(64) González-Rodríguez, D.; Torres, T.; Denardin, E. L. G.; Samios, D.; Stefani, V.; Corręa, D. S. *J. Organomet. Chem.* **2009**, *694* (11), 1617−1622.
(65) Yamasaki, Y.; Mori, T. *Chem. Lett.* **2010**, *39* (10), 1108−1109.
(66) Brisson, E. R. L.; Paton, A. S.; Morse, G. E.; Bender, T. P. *Ind. Eng. Chem. Res.* **2011**, *50* (19), 10910−10917.
(67) Ferro, V. R.; Poveda, L. A.; Claessens, C. G.; Gonzalez-Jonte, R. H.; de la Vega, J. M. G. *Int. J. Quantum Chem.* **2003**, *91* (3), 369−375.
(68) Camerel, F.; Ulrich, G.; Retailleau, P.; Ziessel, R. *Angew. Chem., Int Ed.* **2008**, *47* (46), 8876−80.
(69) Geyer, M.; Plenzig, F.; Rauschnabel, J.; Hanack, M.; Del Rey, B.; Sastre, A.; Torres, T. *Synthesis* **1996**, *1996* (9), 1139−1151.
(70) del Rey, B.; Martínez-Díaz, M.; Barberá, J.; Torres, T. *J. Porphyrins Phthalocyanines* **2000**, *4* (5), 569−573.
(71) Paton, A. S.; Morse, G. E.; Castelino, D.; Bender, T. P. *J. Org. Chem.* **2012**, *77* (5), 2531−6.
(72) Paton, A. S.; Lough, A. J.; Bender, T. P. *Cryst. Eng. Comm.* **2011**, *13* (11), 3653−3656. Paton, A. S.; Morse, G. E.; Lough, A. J.; Bender, T. P. *Cryst. Eng. Comm.* **2011**, *13* (3), 914−919.
(73) Kazmaier, P. M.; Hoffmann, R. *J. Am. Chem. Soc.* **1994**, *116* (21), 9684−9691. Anthony, J. E.; Brooks, J. S.; Eaton, D. L.; Parkin, S. R. *J. Am. Chem. Soc.* **2001**, *123* (38), 9482−3.
(74) Pandey, R.; Gunawan, A. A.; Mkhoyan, K. A.; Holmes, R. J. *Adv. Funct. Mater.* **2012**, *22* (3), 617−624.
(75) Gommans, H.; Verreet, B.; Rand, B. P.; Muller, R.; Poortmans, J.; Heremans, P.; Genoe, J. *Adv. Funct. Mater.* **2008**, *18* (22), 3686−3691.
(76) Hancox, I.; Sullivan, P.; Chauhan, K.; Beaumont, N.; Rochford, L.; Hatton, R.; Jones, T. *Org. Electron.* **2010**, *11* (12), 2019−2025.
(77) Pandey, R.; Holmes, R. J. *Adv. Mater.* **2010**, *22* (46), 5301−5.
(78) Kumar, H.; Kumar, P.; Bhardwaj, R.; Sharma, G. D.; Chand, S.; Jain, S. C.; Kumar, V. *J. Phys. D: Appl. Phys.* **2009**, *42* (1), 015103.
(79) Kippelen, B.; Bredas, J. L. *Energy Environ. Sci.* **2009**, *2* (3), 251−261.
(80) Luhman, W. A.; Holmes, R. J. *Adv. Funct. Mater.* **2011**, *21* (4), 764−771.
(81) Lunt, R. R.; Giebink, N. C.; Belak, A. A.; Benziger, J. B.; Forrest, S. R. *J. Appl. Phys.* **2009**, *105* (5), 053711−053711−7.
(82) Yoo, S.; Domercq, B.; Kippelen, B. *Appl. Phys. Lett.* **2004**, *85* (22), 5427−5429.
(83) Kurrle, D.; Pflaum, J. *Appl. Phys. Lett.* **2008**, *92* (13), 133306.
(84) Yang, J.; Schumann, S.; Hatton, R.; Jones, T. *Org. Electron.* **2010**, *11* (8), 1399−1402. Tong, X. R.; Lassiter, B. E.; Forrest, S. R. *Org. Electron.* **2010**, *11* (4), 705−709.
(85) Hancox, I.; Rochford, L. A.; Clare, D.; Sullivan, P.; Jones, T. S. *Appl. Phys. Lett.* **2011**, *99* (1), 013304.
(86) Pegg, L. J.; Schumann, S.; Hatton, R. A. *ACS Nano* **2010**, *4* (10), 5671−8.
(87) Tress, W.; Petrich, A.; Hummert, M.; Hein, M.; Leo, K.; Riede, M. *Appl. Phys. Lett.* **2011**, *98*, 063301.
(88) Greiner, M. T.; Helander, M. G.; Tang, W.-M.; Wang, Z.-B.; Qiu, J.; Lu, Z.-H. *Nat. Mater.* **2012**, *11* (1), 76−81.
(89) Sarangerel, K.; Ganzorig, C.; Fujihira, M.; Sakomura, M.; Ueda, K. *Chem. Lett.* **2008**, *37* (7), 778−779.
(90) Kulshreshtha, C.; Choi, J. W.; Kim, J. K.; Jeon, W. S.; Suh, M. C.; Park, Y.; Kwon, J. H. *Appl. Phys. Lett.* **2011**, *99* (2), 023308.
(91) Tang, M. L.; Oh, J. H.; Reichardt, A. D.; Bao, Z. *J. Am. Chem. Soc.* **2009**, *131* (10), 3733−40.
(92) Ohno-Okumura, E.; Sakamoto, K.; Kato, T.; Hatano, T.; Fukui, K.; Karatsu, T.; Kitamura, A.; Urano, T. *Dyes Pigm.* **2002**, *53* (1), 57−65.
(93) Verreet, B.; Rand, B. P.; Cheyns, D.; Hadipour, A.; Aernouts, T.; Heremans, P.; Medina, A.; Claessens, C. G.; Torres, T. *Adv Energy Mater* **2011**, *1* (4), 565−568.
(94) Chen, Y. H.; Chang, Y. J.; Lee, G. R.; Chang, J. H.; Wu, I.; Fang, J. H.; Hsu, S. H.; Liu, S. W.; Wu, C. I.; Pi, T. W. *Org. Electron.* **2010**, *11* (3), 445−449.
(95) Chen, Y. H.; Cheng, Y. J.; Lee, G. R.; Wu, C. I.; Pi, T. W. *Org. Electron.* **2011**, *12* (4), 562−565.
(96) Nishi, T.; Kanai, K.; Ouchi, Y.; Willis, M. R.; Seki, K. *Chem. Phys. Lett.* **2005**, *414* (4−6), 479−482.
(97) Kobayashi, N.; Kondo, R.; Nakajima, S.; Osa, T. *J. Am. Chem. Soc.* **1990**, *112* (26), 9640−9641. Kobayashi, N.; Ishizaki, T.; Ishii, K.; Konami, H. *J. Am. Chem. Soc.* **1999**, *121* (39), 9096−9110.
(98) Sastre, A.; Torres, T.; Diaz-Garcia, M. A.; Agullo-Lopez, F.; Dhenaut, C.; Brasselet, S.; Ledoux, I.; Zyss, J. *J. Am. Chem. Soc.* **1996**, *118* (11), 2746−2747.
(99) Claessens, C. G.; Gonzalez-Rodriguez, D.; del Rey, B.; Torres, T.; Mark, G.; Schuchmann, H. P.; von Sonntag, C.; MacDonald, J. G.; Nohr, R. S. *Eur. J. Org. Chem.* **2003**, 2547−2551.
(100) Paton, A. S. L., A.J.; Bender, T. P. *Ind. Eng. Chem. Res.* **2012**, *51*, 6290−6296.
(101) Tolbin, A. Y.; Tomilova, L. G. *Russ. Chem. Rev.* **2011**, *80* (6), 531−551.
(102) Potz, R.; Göldner, M.; Hückstädt, H.; Cornelissen, U.; Tutaß, A.; Homborg, H. *Z. Anorg. Allg. Chem.* **2000**, *626* (2), 588−596.
(103) Zyskowski, C. D.; Kennedy, V. O. *J. Porphyrins Phthalocyanines* **2000**, *4* (7), 649−654.
(104) Guilleme, J.; Gonzalez-Rodriguez, D.; Torres, T. *Angew. Chem., Int. Ed.* **2011**, *50* (15), 3506−3509.
(105) Yamasaki, Y.; Mori, T. *Bull. Chem. Soc. Jpn.* **2011**, *84* (11), 1208−1214.

(106) Ziessel, R.; Ulrich, G.; Elliott, K. J.; Harriman, A. *Chem.—Eur. J.* **2009**, *15* (20), 4980−4984.
(107) Mori, T.; Yamasaki, Y. , U.S. Patent 8 105 431, 2009.
(108) Yamasaki, Y.; Mori, T. *Bull. Chem. Soc. Jpn.* **2012**, *85* (2), 245−247.
(109) Kato, T.; Tham, F. S.; Boyd, P. D. W.; Reed, C. A. *Heteroatom Chem.* **2006**, *17* (3), 209−216.
(110) Hanack, M.; Geyer, M. *J. Chem. Soc., Chem. Commun.* **1994**, *19*, 2253−2254.
(111) Díaz, D. D.; Bolink, H. J.; Cappelli, L.; Claessens, C. G.; Coronado, E.; Torres, T. *Tetrahedron Lett.* **2007**, *48* (27), 4657−4660.
(112) Lapok, L.; Claessens, C. G.; Wohrle, D.; Torres, T. *Tetrahedron Lett.* **2009**, *50* (18), 2041−2044.
(113) Morse, G. E.; Gantz, J. L.; Steirer, K. X.; Armstrong, N. R.; Bender, T. P. **2012**, unpublished.
(114) Agrawal, A. K.; Jenekhe, S. A. *Chem. Mater.* **1996**, *8*, 579−589.